chemistry

MDPI

Review

The Application of DNA Origami in Biosensing

Renjie Niu [1,*,†], Mengyao Tao [1,†] and Jie Chao [2]

[1] School of Medical Imaging, Xuzhou Medical University, Xuzhou 221004, China; 18151134330@163.com
[2] State Key Laboratory for Organic Electronics and Information Displays & Jiangsu Key Laboratory for Biosensors, Institute of Advanced Materials (IAM), Jiangsu National Synergistic Innovation Center for Advanced Materials (SICAM), Nanjing University of Posts and Telecommunications, Nanjing 210023, China; iamjchao@njupt.edu.cn
* Correspondence: iamrjniu@163.com
† These authors contributed equally to this work.

Abstract

Biosensing plays a vital role in medical diagnostics, environmental monitoring, and food safety, enabling highly sensitive and specific detection of diverse biological and chemical targets. However, conventional biosensing platforms still suffer from limited sensitivity, poor nanoscale resolution, and restricted multiplexed or dynamic detection capabilities. DNA origami, as an emerging bottom-up nanofabrication strategy, enables the construction of programmable nanostructures with high spatial precision. This capability allows the rational arrangement of functional molecules at the nanoscale, thereby offering significant advantages for biosensing applications. Specifically, DNA origami can enhance signal amplification, improve spatial resolution, and enable multiplexed detection under complex conditions. In this review, we provide a systematic overview of recent advances in the application of DNA origami across various classes of biosensors, including microscopy-based biosensors, nanopore biosensors, electrochemical biosensors, fluorescent biosensors, SERS biosensors, and other related biosensors. We aim for this review to advance the development of DNA origami-based biosensing and to provide new insights for researchers working in related fields.

Keywords: DNA origami; biosensors; nanopore; electrochemistry; fluorescence; surface-enhanced Raman spectroscopy



Academic Editor: Michael Lyons

Received: 31 August 2025
Revised: 27 September 2025
Accepted: 2 October 2025
Published: 10 October 2025

Citation: Niu, R.; Tao, M.; Chao, J. The Application of DNA Origami in Biosensing. *Chemistry* **2025**, *7*, 165. https://doi.org/10.3390/chemistry7050165

Copyright: © 2025 by the authors. Licensee MDPI, Basel, Switzerland. This article is an open access article distributed under the terms and conditions of the Creative Commons Attribution (CC BY) license (https://creativecommons.org/licenses/by/4.0/).

1. Introduction

Biosensors, which integrate biological recognition elements with physical or chemical transduction methods, enable highly sensitive and specific detection of diverse targets such as pathogens [1,2], nucleic acids [3,4], proteins [5], and molecules [6]. These capabilities provide reliable tools for early disease diagnosis, environmental pollution monitoring, and food quality control. With the growing demands of precision medicine [7,8] and public health security, the development of novel, high-performance biosensing technologies has become an important focus in both research and practical applications.

Despite remarkable progress achieved by conventional biosensing platforms, several limitations remain. For example, classical electrochemical biosensors, such as enzyme electrodes first proposed by Clark and Lyons in 1962, have become widely used in glucose monitoring [9,10]. However, in complex biological samples, enzyme activity is often unstable, and nonspecific interactions can compromise sensitivity and reproducibility [11,12]. Similarly, traditional nanopore sensing technologies allow single-molecule detection but

face difficulties in precise control over channel construction and in achieving high target selectivity [13,14].

To address these challenges, DNA origami has emerged as a powerful bottom-up nanofabrication technique [15]. Through rational sequence design, DNA origami enables the construction of controllable, spatially well-defined three-dimensional (3D) structures at the nanoscale [16–18]. Such nanostructures provide highly programmable platforms for the precise positioning of functional molecules, thereby facilitating fine-tuned and controllable biosensing with improved specificity and stability. In recent years, DNA origami has demonstrated broad potential in various biosensing applications. In this review, we categorize DNA origami-based biosensors according to their signal output modalities and systematically discuss their recent advances. Specifically, we highlight microscopy-based biosensors, nanopore biosensors, electrochemical biosensors, fluorescent biosensors, and surface-enhanced Raman spectroscopy (SERS) biosensors, among others, while also addressing their advantages and current challenges.

2. DNA Origami-Based Biosensors

2.1. Microscopy-Based Biosensors

Microscopic characterization techniques are among the most essential analytical tools in fields such as nanomaterials research and nanotechnology, aiming to directly observe and quantitatively analyze the morphology, structure, composition, and properties of objects at the micro- and nanoscale [19]. These techniques achieve high-resolution imaging and structural analysis beyond the diffraction limit of conventional optical microscopy by exploiting interactions between probes and samples, or between electrons/photons and materials. Commonly employed methods include atomic force microscopy (AFM) [20,21], transmission electron microscopy (TEM) [22], and scanning electron microscopy (SEM) [23,24]. AFM, a technique of scanning probe microscopy, obtains 3D morphological information of samples by detecting nanoscale interaction forces between the probe tip and the sample surface. TEM, in contrast, utilizes high-energy electrons transmitted through samples to directly resolve internal microstructures, achieving sub-nanometer to even atomic-scale resolution. Therefore, microscopy-based characterization techniques have become ideal tools for signal readout in DNA origami-based biosensors. With the continuous advancement of DNA origami, numerous biosensors employing microscopy-based readout have been developed for the detection of various targets [25–30].

In 2008, Ke et al. first realized AFM-based biosensors by using rectangular DNA origami carrying specific probe sequences to detect RNA molecules. The designed probes could hybridize with target RNAs, and upon binding, the local structure became stiffer, which could then be directly observed by AFM, thereby enabling label-free detection. The study demonstrated specific detection of multiple RNAs, and the method remained effective even in complex cellular RNA environments (Figure 1A) [31]. In recent years, new types of AFM-based biosensors have been developed for RNA detection [32]. Zhu et al. immobilized probes on two-dimensional (2D) DNA origami and attached them to quantum dot-labeled markers. When the target miRNA (such as miRNA-133) was present, it initiated a strand displacement reaction that replaced the probe–quantum dot complexes, causing the originally visible bright spots on the origami surface to disappear. By directly counting the changes in these bright spots using AFM, they established a linear relationship between miRNA concentration and the detection signal [33]. Kuzuya et al. developed microRNA detection using dynamic 3D DNA origami. They designed the DNA origami into plier-like devices that can switch between “open” and “closed” states, with specific probes positioned at the “jaws.” Upon the presence of microRNA, binding to these probes induces the transition of the DNA pliers from an open cross-shaped form to a closed

state. The structural changes in the DNA pliers are directly visualized by AFM, allowing the detection of target molecules and the evaluation of their binding strength [34].

Similarly, this type of AFM-based biosensor can also be applied to DNA detection [35,36]. Recently, Xiong et al. employed DNA origami combined with AFM to detect and localize DNA repetitive sequences. In this approach, DNA origami serves as "nano-tags," where specially designed tri-block structures connect target repetitive sequences with differently shaped DNA origami, enabling direct visualization of their precise positions and spacing on gene templates under AFM. This strategy not only allows nanoscale discrimination of different repetitive sequences but also enables simultaneous detection of multiple repeats with a resolution of ~6.5 nm (equivalent to 19 nucleotides). Compared with traditional sequencing (typical optical mapping resolution of about 100–1000 nm) or fluorescence imaging (diffraction-limited resolution of ~200 nm), this method achieves a ~30–300-fold improvement in resolution, while offering simpler operation and lower cost, thus providing a powerful tool for gene mapping and the study of genetic disease mechanisms (Figure 1B) [37].

These approaches can also be extended to the detection of single-nucleotide polymorphisms (SNPs) [38]. In 2010, Zhang et al. anchored specific DNA probes onto 2D DNA origami. In the presence of a perfectly matched target DNA, a strand-displacement reaction was initiated, leading to the replacement of the pre-hybridized reporter strand and the consequent disappearance of streptavidin features in AFM imaging. In contrast, when the target DNA contained a single-base mismatch, the displacement efficiency was markedly reduced, and the bright spots remained visible. This strategy enabled label-free and room-temperature discrimination of SNP variants, providing a highly specific platform for genotyping [39]. By the same principle, Seeman's group arranged letter-shaped patterns on DNA origami to detect SNPs. When the DNA probe is fully complementary to the sequence on the origami, the corresponding letter is erased; if there is a single base mismatch, the letter remains [40]. Zhang et al. folded DNA origami into different shapes that function like "magnifying lenses" under the microscope to help identify SNPs. They analyzed genetic variations in the human genome by first allowing these origami tags to specifically bind to different positions on the target DNA, and then directly observing their shapes and distributions along the DNA using AFM. In this way, they were able not only to clearly distinguish different genotypes at the nanoscale but also to analyze multiple loci simultaneously, thereby achieving high-resolution single-molecule genotyping and haplotyping (Figure 1C) [41].

Apart from nucleic acids, microscopy-based biosensors can also be used to detect pH [42]. Zhang and colleagues designed a DNA origami nanocaliper that functions like a tiny ruler capable of opening and closing. On the two arms of this structure, they incorporated pH-responsive triplex DNA. When the environmental pH changes, the triplex DNA undergoes structural transitions that alter the hinge angle of the nanocaliper. By directly observing these angular changes using TEM, the local pH can be determined with a resolution of 0.1 pH units, representing a ~5–10-fold improvement compared to conventional pH-sensitive fluorescent probes (typical resolution ~0.5–1 pH units). Using this approach, they further examined whether there were local pH variations near carbon nanotubes, and the results demonstrated that this DNA origami device can sensitively probe acidity at the nanoscale [43].

In addition, microscopy-based biosensors can also be used to monitor dynamic changes [44]. Voigt et al. employed DNA origami as a nanoscale reaction platform, where different functional groups were pre-positioned, and single-molecule chemical reactions were directly visualized using AFM [45]. Tintoré et al. anchored specific aptamer sequences onto DNA origami, enabling them to selectively recognize and bind thrombin molecules.

By directly observing the morphological differences on the origami surface with or without the target protein using AFM, they achieved label-free, single-molecule level detection of thrombin binding events [46]. Endo and colleagues constructed a DNA origami frame that allows the precise placement of double-stranded DNA and enables control over its tension, orientation, and topology. Using this system, they directly imaged and analyzed a variety of biological processes at subsecond time resolution, including DNA methylation, DNA repair, recombination, RNA polymerase transcription, G-quadruplex formation and disruption, hybridization and dissociation of photoresponsive oligonucleotides, B–Z conformational transition, and the movement of DNA nanomachines along a track [47]. Recently, Prakash et al. precisely arranged gold nanoparticles (AuNPs) on 3D DNA origami rods to create unique barcode patterns. These barcodes were introduced to specific antigen sites in tissue sections through hybridization with modified antibodies, enabling high-contrast and distinguishable labeling under TEM. The study demonstrated two different DNA origami designs, distinct antibody modification strategies, and successfully labeled opsin and recoverin proteins in mouse retina sections (Figure 1D) [48].

However, microscopy-based biosensors heavily rely on advanced instruments such as AFM and TEM, which are not only costly and technically demanding to operate but also require region-by-region scanning for each measurement, resulting in extremely low throughput that is insufficient for large-scale screening. Impurities in complex biological samples can generate background noise and interfere with signal recognition, while in dynamic detection, the trade-off between imaging speed and structural stability, along with operator-dependent interpretation that leads to quantitative bias, further limits their practical applications.

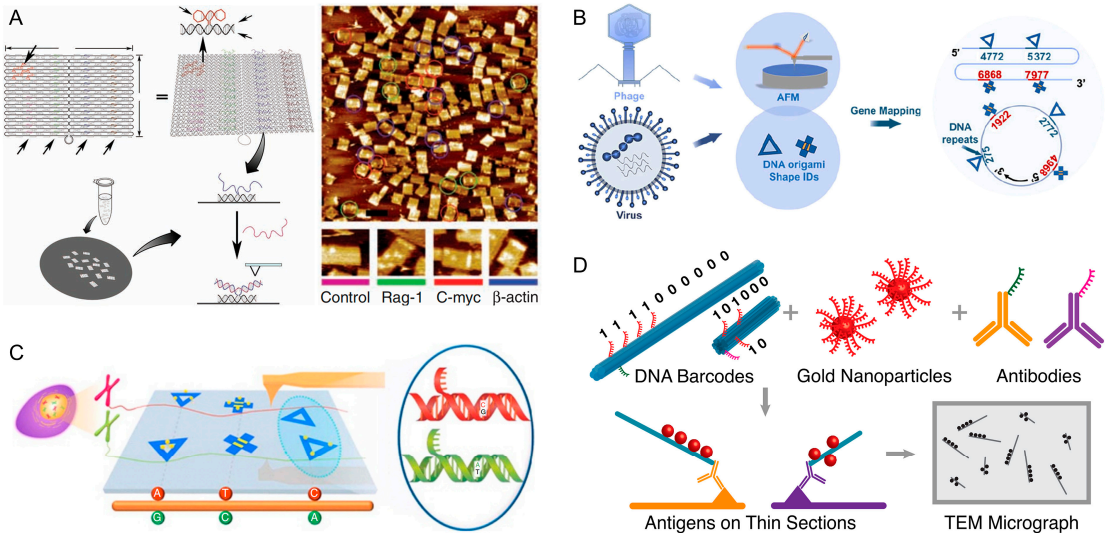


Figure 1. Microscopy-based biosensors enabled by DNA origami. (**A**) Rectangular DNA origami tiles display multiple capture probes with nanometer precision, and target binding stiffens the probe regions to produce clear AFM signals, enabling label-free RNA detection [31]. Reproduced from Science, with permission from The American Association for the Advancement of Science, 2008. (**B**) Tri-block DNA structures connect repetitive sequences to origami tags for AFM visualization, enabling precise gene mapping with ~6.5 nm resolution [37]. Reproduced from Journal of the American Chemical Society, with permission from American Chemical Society, 2024. (**C**) DNA origami functions like "magnifying lenses" under the AFM to help identify SNPs [41]. Reproduced from Nature Communications, with permission from Springer Nature, 2017. (**D**) AuNP-decorated DNA origami served as modular barcodes that hybridize to DNA-modified antibodies for TEM imaging, enabling multiplexed antigen detection in tissue sections [48]. Reproduced from ACS Applied Materials & Interfaces, with permission from American Chemical Society, 2025.

2.2. Nanopore Biosensors

Nanopore biosensors are analytical tools that enable single-molecule detection [49,50]. Their working principle is that when an individual biomolecule (such as DNA) passes through a nanoscale pore, it induces measurable characteristic changes in the ionic current. The key advantage of this technology is that it enables real-time, high-throughput single-molecule analysis without the need for fluorescent or radioactive labeling. DNA origami technology enables the fabrication of nanopores with customizable and tunable dimensions, while precisely controlling the positioning of target-responsive probes.

In 2011, Bell et al. first combined DNA origami with solid-state silicon nitride nanopores to construct hybrid nanopores that could be repeatedly inserted and ejected. They designed a DNA origami structure with interlaced double helices featuring a central channel of 7.5 × 7.5 nm^2, and employed a double-stranded DNA overhang to guide voltage-driven self-assembly into silicon nitride pores with diameters of 13–18 nm. The resulting hybrid nanopores exhibited rectification effects in current–voltage curves and enabled the detection of λ-DNA molecules through ionic current blockade [51]. In the following years, a number of nanopore biosensors based on DNA origami were developed for DNA detection [52,53]. In 2013, Hernández-Ainsa et al. combined DNA origami with glass nanocapillaries to build a reversibly controlled hybrid nanopore. They confirmed the trapping of DNA origami at the capillary tip using single-molecule fluorescence imaging together with ionic current measurements. The authors demonstrated two applications of this nanopore: first, by tuning the pore size in the DNA origami, they achieved physical control over the folding and translocation of λ-DNA, with a translocation time precision of ±5 ms—approximately 20-fold higher than that of unmodified glass nanocapillaries; second, by introducing sequence-specific single-stranded DNA overhangs at the pore entrance, they realized chemical control for the selective recognition of target ssDNA (Figure 2A) [54].

In addition to DNA detection, nanopore biosensors integrated with DNA origami can also be applied to protein analysis. Raveendran et al. designed a "carrier–cavity" DNA origami structure for the detection of low-abundance proteins by functionalizing the cavity with a CRP-specific DNA aptamer. Upon CRP binding, the translocation signal shifted from a double-current peak (amplitude 65 ± 6 pA, dwell time 0.29 ± 0.1 ms) to a single-current peak (amplitude 90 ± 9 pA, dwell time 0.15 ± 0.05 ms). The system achieved detection limits of 3 nM in buffer, 9 nM in 5% human plasma, 12 nM in 10% human serum, and 15 nM in filtered urine (pH 6.0–7.0), all within clinically relevant CRP ranges (healthy: <8 nM; inflammation: >8 μM). In terms of anti-interference performance, the sensor exhibited negligible cross-reactivity toward interfering proteins such as albumin at concentrations over 100-fold higher than CRP, and maintained signal stability in the presence of 5 mM glucose or 100 μM uric acid. Moreover, the use of a 95% confidence ellipse classification based on multiparametric features effectively eliminated false positives. A key advantage of this system lies in its resistance to protein fouling: the 95 × 95 nm^2 two-dimensional origami frame minimized exposed single-stranded regions, while the negatively charged phosphate backbone was shielded by neutral oligonucleotide "spacers," resulting in only ~12% protein adsorption after 2 h incubation in 50% plasma (compared with ~45% for linear DNA carriers). In terms of stability, more than 85% structural integrity was retained after 7 days at 4 °C in buffer, and ~70% activity was preserved after 4 h in 5% plasma at 37 °C. Batch-to-batch reproducibility tests further demonstrated relative standard deviations (RSDs) below 10% for peak amplitude, below 15% for dwell time, and below 8% for the detection limit in 5% plasma (Figure 2B) [55].

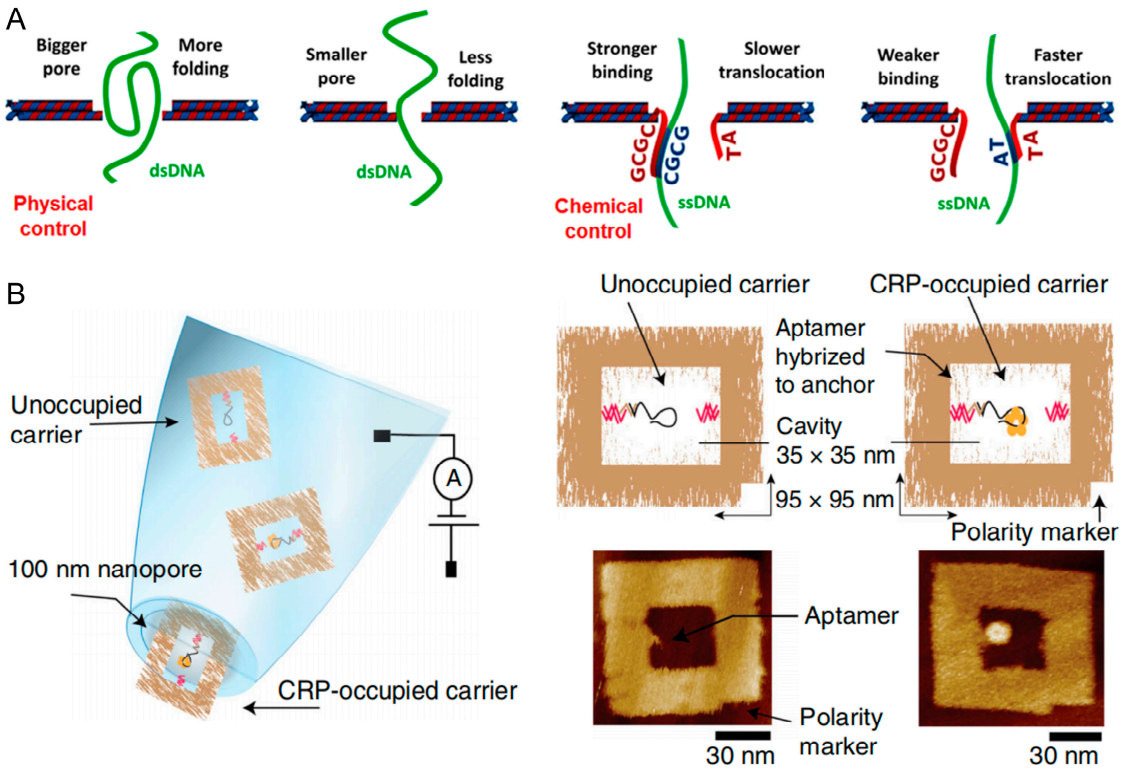


Figure 2. Nanopore biosensors enabled by DNA origami. (**A**) DNA origami sheets with central pores were voltage-trapped onto glass nanocapillaries to form reversible hybrid nanopores. These nanopores allow controlled DNA translocation and sequence-selective ssDNA detection [54]. Reproduced from ACS Nano, with permission from American Chemical Society, 2013. (**B**) Frame-shaped origami with central cavities were functionalized with CRP-specific aptamers and analyzed by nanopipette translocation. Occupied and unoccupied carriers showed distinct ion current fingerprints [55]. Reproduced from Nature Communications, with permission from Springer Nature, 2020.

Recently, Long et al. developed a reconfigurable DNA origami hinge for nanopore-based detection of microRNAs. The hinge was designed to undergo a conformational transition from a closed to an extended state upon binding to miRNA-141-3p, a biomarker associated with prostate cancer, thereby generating distinct ionic current signatures during nanopore translocation that enabled single-molecule level detection. The method demonstrated sensitivity down to the nanomolar range and exhibited excellent selectivity, effectively discriminating highly similar miRNA sequences. Moreover, reliable performance was achieved in diluted human serum samples, highlighting both stability and specificity. This work underscores the potential of DNA nanostructure-enabled nanopore sensing for highly sensitive and selective biomarker detection [56].

Although nanopore biosensors offer numerous advantages, several limitations remain. Hybrid nanopore structures are prone to ionic perturbations in physiological environments, leading to deformation; the resolution of translocation signals is often insufficient; and highly homologous target molecules can easily produce false positives. In addition, sample preprocessing is cumbersome, pore size cannot be dynamically tuned, and large-scale fabrication suffers from poor uniformity and limited long-term durability, making it difficult to accommodate diverse detection requirements or repeated use scenarios.

2.3. Electrochemical Biosensors

Electrochemical biosensors are analytical devices that integrate biological recognition elements (such as antibodies, nucleic acids, or enzymes) with electrochemical detection techniques, with their core function being the conversion of specific biomolecular inter-

actions (e.g., antigen–antibody binding or nucleic acid hybridization) into quantifiable electrical signals such as changes in current, voltage, or resistance [57,58]. These biosensors offer multiple advantages, including low power consumption, ease of miniaturization, and compatibility with portable electronic readout, which are highly relevant for the development of practical and portable biosensing devices. In recent years, efforts have been made to couple DNA origami technology with electrochemical detection, where precise control over nanoscale structural configuration, probe density, and signal molecule distribution has enabled substantial improvements in sensitivity, selectivity, and practical applicability.

Electrochemical sensors based on DNA origami are commonly employed for the detection of nucleic acids. In 2019, Han et al. employed a cross-shaped DNA origami structure as a probe carrier, in which single-stranded DNA probes were positioned at predefined sites and immobilized onto a gold electrode surface via electrostatic adsorption of chitosan. Using methylene blue (MB) as a redox indicator, this system enabled label-free detection of microRNA-21 [59]. Paul Williamson and colleagues focused on signal amplification strategies to advance DNA origami-based sensors toward higher sensitivity. Exploiting the programmable assembly of DNA origami, they constructed a pegboard-like structure and employed a sandwich assay to capture the blaOXA-1 gene fragment on the electrode surface. Changes in charge transfer resistance (RCT) were subsequently monitored using electrochemical impedance spectroscopy (EIS), thereby achieving effective signal amplification. Compared with conventional label-free sensors, this method lowers the detection limit from 3.22 nM to 8.86 pM, representing an approximately 363-fold enhancement in sensitivity [60]. Recently, Qin et al. integrated DNA origami with other functional materials, including peptide nucleic acids (PNA) and gold nanostructures, to develop a portable platform for the detection of circulating tumor DNA (ctDNA). In this strategy, DNA origami captures ctDNA in solution to form complexes, which are subsequently immobilized on the electrode surface through the synergistic effects of PNA—providing charge neutrality to minimize background noise—and gold nanostructures—offering a high surface area for enhanced loading. Furthermore, the intrinsic negative charge of DNA origami enables the adsorption of $[Ru(NH_3)_6]^{3+}$, thereby achieving effective signal amplification (Figure 3A) [61].

The application of DNA origami in electrochemical biosensors extends beyond nucleic acid detection to include protein analysis. Byoung-jin Jeon et al. employed a modular DNA origami system capable of "open–closed" conformational switching, coupled with square wave voltammetry (SWV), to achieve highly sensitive detection of single-stranded DNA, streptavidin, and platelet-derived growth factor BB (PDGF-BB). The key breakthrough of this work lies in the remarkable enhancement of signal transduction efficiency, with a signal gain of up to 1270% for ssDNA detection and a detection limit below 1 pM for streptavidin, approximately 1000-fold lower than conventional electrochemical protein sensors. By integrating the structural dynamics of DNA origami with advanced electrochemical signal conversion, this study successfully overcame the longstanding limitations of weak signals and low gain in conventional sensors, establishing a versatile platform for multi-target detection [62]. Electrochemical sensors based on DNA origami can also be employed to monitor dynamic reaction processes. Fan and colleagues immobilized rectangular DNA origami structures on a gold electrode surface and assembled glucose oxidase (GOx) and horseradish peroxidase (HRP) into a cascade enzyme system on the origami scaffold to probe their reaction dynamics. By precisely controlling the spatial distance between the two enzymes, they were able to quantitatively elucidate the distance-dependent behavior of enzymatic activity (Figure 3B) [63].

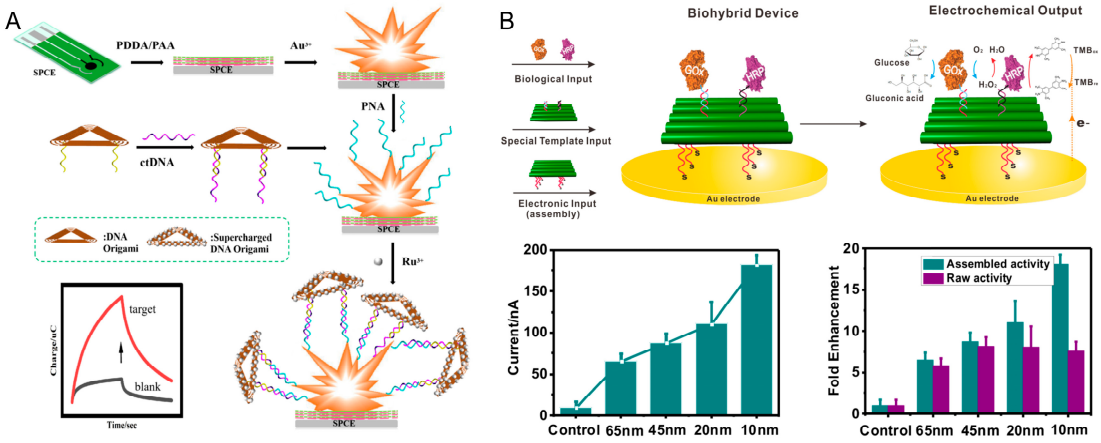


Figure 3. Electrochemical biosensors enabled by DNA origami. (**A**) Triangular DNA origami carriers hybridize with PNA probes on gold nanostructures and enrich electroactive molecules, greatly amplifying signals for ultrasensitive and specific ctDNA detection [61]. Reproduced from Biosensors & Bioelectronics, with permission from Elsevier, 2025. (**B**) Rectangular origami scaffolds positioned glucose oxidase and horseradish peroxidase at controlled distances and anchored them onto gold electrodes. The spatially organized cascade produced distance-dependent electrochemical readouts, demonstrating efficient wiring of redox enzymatic pathways [63]. Reproduced from ACS Applied Materials & Interfaces, with permission from American Chemical Society, 2018.

It is evident that DNA origami-based electrochemical biosensors offer advantages such as multifunctionality and high spatial precision. However, they also face several limitations. The stability of electrode modification is often poor, with DNA origami structures prone to detachment in biological fluids. Electroactive substances present in biological samples, together with the intrinsic charge properties of DNA origami, can interfere with the signals and cause background drift. Signal amplification strategies require a trade-off between complexity and efficiency, while miniaturization and integration remain challenging. Furthermore, multiplexed detection is prone to crosstalk, long-term storage stability is insufficient, and clinically applicable preservation protocols are still lacking.

2.4. Fluorescent Biosensors

Fluorescent biosensors have emerged as powerful tools in biological detection and disease diagnostics owing to their high sensitivity, real-time imaging capability, and operational simplicity [64,65]. DNA origami, as a highly programmable nanoscale platform, provides unique opportunities for precise modulation and efficient transduction of fluorescent signals. By spatially arranging fluorophores, quenchers, or aptamer probes with nanoscale accuracy on DNA origami scaffolds [66], these systems enable the specific recognition of diverse targets such as nucleic acids, proteins, and small molecules, while significantly enhancing signal amplification and spatial resolution. This programmability gives DNA origami-based fluorescent sensors unique advantages, making them strong candidates for next-generation biosensing technologies.

This technique can be applied to nucleic acid detection [67,68]. In earlier work, Zadegan et al. designed and assembled a hollow DNA box whose lid could be repeatedly opened and closed by a specific "molecular key." This switchable structure, based on a DNA strand displacement mechanism, was engineered to respond to breast cancer-related microRNA, thereby enabling controlled opening of the nanobox. The structure and its dynamic behavior were characterized using gel electrophoresis, dynamic light scattering, AFM, TEM, and fluorescence resonance energy transfer (FRET) spectroscopy [69]. Domljanovic et al. developed a dynamic DNA origami "book" biosensor capable of single or dual detection of cancer-related nucleic acids through FRET or fluorescence quenching mechanisms. The sen-

sor was functionalized with arrays of fluorophores, acceptors, and quenchers, where target binding induced structural rotation that led to decreased FRET efficiency or increased fluorescence intensity. At the single-molecule level, this system can simultaneously detect two targets within 10 min, with a detection limit of 1–10 pM—approximately 100–1000 times lower than that of conventional fluorescent nucleic acid sensors—and has been successfully applied to both synthetic oligonucleotides and endogenous microRNAs extracted from cancer cells [70].

As research has progressed, attention has expanded beyond nucleic acids to other biomolecules, with several studies employing fluorescent biosensors for protein detection [71,72]. Ke and colleagues developed a rhombus-shaped DNA origami nanoactuator that integrates with split eGFP to form a DNA–protein hybrid nanostructure, which functions as a biosensor by transducing long-range conformational changes into tunable fluorescence signals in response to external stimuli such as buffer composition, restriction enzymes, and specific nucleic acids [73]. In 2018, Domljanovic et al. designed and synthesized a series of dihydropyridine (DHP)-based fluorophores capable of forming stable complexes with double-stranded DNA and generating fluorescence changes in the presence of anti-DNA antibodies, such as anti-dsDNA antibodies found in the sera of systemic lupus erythematosus (SLE) patients. The authors systematically evaluated the optical properties and biorecognition capabilities of different DHP derivatives, identified candidates with optimal sensitivity and specificity, and employed DNA origami as an antigen platform to establish a direct immunofluorescence assay. This method was applied to clinical samples and successfully detected antibodies in the sera of 80 SLE patients, achieving a sensitivity of 92.5% and a specificity of 95%, which are higher than those of conventional ELISA (85% and 90%, respectively). Its performance is comparable to traditional ELISA and shows strong correlations with specific clinical features such as arthritis (Figure 4A) [74].

In addition to the commonly targeted DNA and proteins, DNA origami-based fluorescent sensors have also been employed for the detection of various small molecules [75]. Walter et al. reported the detection of ATP molecules using a DNA origami "traffic light" biosensor. In this design, split ATP aptamers were embedded into two lever arms of the origami, each functionalized with a pair of cyanovinyl dye molecules (a green donor and a red acceptor), enabling dual-color readout through FRET. Upon ATP binding, the origami structure switched from an open to a closed conformation, resulting in a fluorescence shift from green to red. AFM imaging confirmed the conformational transition, with the ratio of closed to open states correlating well with the fluorescence ratio. Importantly, the aptamer needed to be positioned furthest from the pivot point to ensure effective detection. The system exhibited high sensitivity within the ATP concentration range of 0.10–1.00 mM [76]. Marras et al. demonstrated ion detection using a DNA origami hinge-based strategy. In this approach, short single-stranded DNA sensitive to cation concentration was incorporated, enabling hinge conformational changes driven by cation-induced affinities (e.g., Mg^{2+}, K^{+}, Na^{+}, Ca^{2+}, Spd^{3+}). By combining single-molecule FRET and TEM analysis, the system achieved sub-second response times. Furthermore, through statistical mechanics modeling, the design was optimized and shown to discriminate between ions of different valencies [77]. Grabenhorst et al. developed a versatile DNA origami-based modular single-molecule fluorescence sensing platform capable of detecting a wide range of biomolecular targets. By decoupling target recognition from signal output, the system harnesses large conformational changes to generate a high-contrast FRET readout. The authors systematically explored strategies for tuning sensor performance, including the use of multivalency to enhance cooperativity and the modulation of ionic strength and structural stabilization to shift the response window. Furthermore, the platform was successfully extended to diverse targets such as antibodies, proteins, enzymatic activities, and RNA, and was

even engineered to perform multiplexed detection through logic-gate sensing schemes (Figure 4B) [78].

In addition to focusing on various biomolecular targets, researchers have also explored and detected physicochemical properties such as environmental factors, molecular energy, and particle characteristics [79–81]. For example, Hudoba et al. investigated compressive depletion forces using a dynamic DNA origami device. By employing single-molecule FRET and TEM, they were able to probe such forces under molecular crowding conditions. Using polyethylene glycol (PEG) as a crowding agent, this device can detect sub-piconewton depletion forces with a resolution of ~100 fN, representing an approximately 10-fold improvement over conventional force-sensing methods. Moreover, by varying the number of constraining strands, the equilibrium and kinetic behavior could be finely tuned, enabling quantitative measurement of depletion forces across different PEG molecular weights and concentrations [82]. Ijas et al. reported pH sensing using reconfigurable DNA origami nanocapsules. These capsules employed a pH-responsive Hoogsteen triplex DNA "pH-lock" mechanism to achieve reversible opening and closing, which was monitored via FRET using Alexa Fluor 488 as the donor and Alexa Fluor 594 as the acceptor. The nanocapsules exhibited a pKa of approximately 7.27 and responded rapidly to pH changes within the range of 6.4–7.8. They were further shown to encapsulate AuNPs and HRP, with a pH shift as small as 0.5 units sufficient to trigger conformational switching. Importantly, the nanocapsules remained stable under physiological salt conditions, and HRP retained its enzymatic activity upon encapsulation (Figure 4C) [83]. Hemmig et al. constructed a voltage-responsive DNA origami structure labeled with a FRET dye pair (ATTO532 as the donor and ATTO647N as the acceptor). By immobilizing the structure on a nanocapillary and combining ionic current recording with fluorescence imaging, they achieved voltage-dependent detection within the range of 100–400 mV [84]. Ochmann et al. quantitatively investigated membrane surface charges by developing a DNA origami-based sensor. In this design, a charge-sensing unit equipped with fluorescent donor and acceptor pairs was integrated into the origami platform, enabling single-molecule FRET imaging. This approach allowed for sensitive detection of charge variations in differently charged lipid membranes (e.g., large unilamellar vesicles) and provided a powerful method to characterize membrane surface charge distributions with nanoscale resolution [85]. Recently, Büber et al. developed flexible DNA origami-based curvature sensors that, in combination with single-molecule FRET readout, enabled sensitive determination of nanoparticle and lipid vesicle surface curvature and size within the 50–300 nm range [86].

In addition to employing FRET-based strategies for sensing, some studies have utilized surface-enhanced fluorescence to achieve analyte detection [87–90]. The underlying principle relies on localized surface plasmon resonance effects generated near metallic nanostructures, which markedly enhance the excitation and emission efficiency of fluorophores, thereby amplifying the fluorescence signal. Compared with conventional fluorescence detection, this approach enables stronger signal output at lower analyte concentrations, effectively improving both detection sensitivity and signal-to-noise ratio. For example, a recent study from Philip Tinnefeld's group demonstrated a novel amplification-free strategy for ultra-sensitive nucleic acid detection by exploiting surface-enhanced fluorescence. In this work, DNA origami nanoantennas were employed as a single-molecule fluorescence sensing platform to detect a 151-nucleotide sequence specific to antibiotic-resistant *Klebsiella pneumoniae*. By optimizing DNA origami design to achieve nanopatterned arrangements and integrating a microfluidic chip with a low-cost single-molecule fluorescence reader, this system reaches detection limits of 5 aM in buffer and 10 aM in untreated human plasma—approximately 10^6–10^7 times lower than those of conventional PCR-based assays. Moreover, fluorescence enhancement provided a pronounced improvement in signal-to-

background discrimination, while silicification of the structures ensured stability in complex clinical samples. Compared with conventional PCR, LAMP, or CRISPR-based assays, this platform reached comparable or superior sensitivity without enzymatic amplification, while offering reusability and adaptability to diverse nucleic acid targets, thereby presenting a promising solution for rapid and low-cost point-of-care diagnostics (Figure 4D) [91].

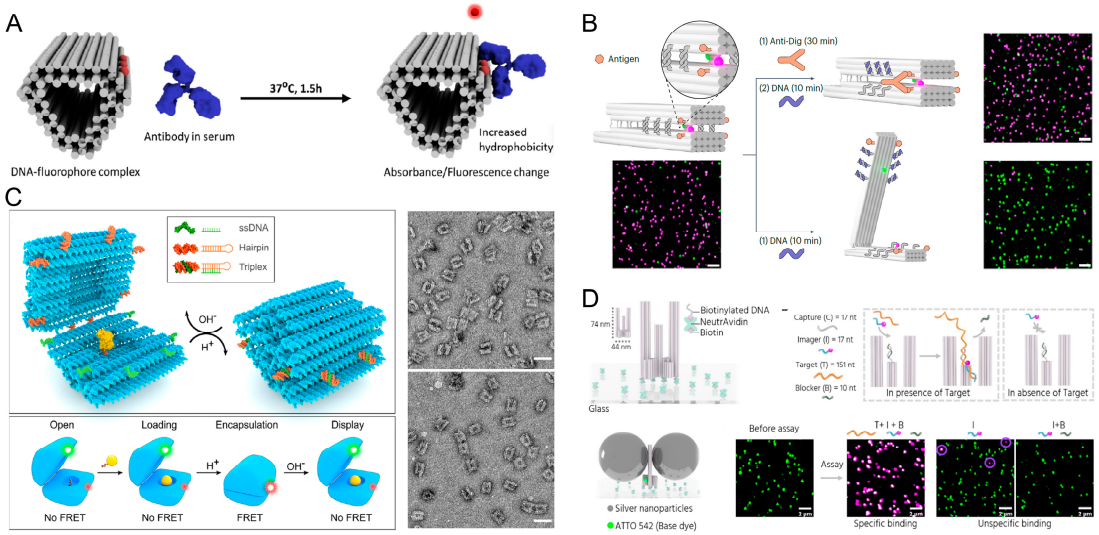


Figure 4. Fluorescent biosensors enabled by DNA origami. (**A**) DNA origami–fluorophore complexes detect serum anti-DNA antibodies via fluorescence change [74]. Reproduced from ACS Omega, with permission from American Chemical Society, 2018. (**B**) Dynamic DNA origami hinges equipped with digoxigenin antigens remained closed upon binding anti-Dig antibodies, producing high-contrast FRET signals. This modular platform demonstrated reliable single-molecule antibody sensing [78]. Reproduced from Nature Nanotechnology, with permission from Springer Nature, 2024. (**C**) DNA origami capsules with triplex "pH latches" reversibly open and close, enabling controlled cargo encapsulation and release [83]. Reproduced from ACS Nano, with permission from American Chemical Society, 2019. (**D**) DNA origami nanoantennas detect antibiotic-resistant Klebsiella pneumoniae DNA sequences via surface fluorescence enhancement [91]. Reproduced from Advanced Materials, with permission from Wiley-VCH, 2025.

DNA origami-based fluorescent biosensors, owing to their high temporal resolution, enable real-time imaging and exhibit considerable structural design flexibility, while fluorescence-enhancement-based sensors can markedly improve detection sensitivity. However, DNA origami-based fluorescent biosensors still encounter multiple challenges: their signals are prone to photobleaching and interference from sample autofluorescence, leading to reduced sensitivity in complex matrices such as whole blood; in live-cell environments, DNA origami structures are susceptible to nuclease-mediated degradation, resulting in insufficient stability; moreover, in multiplexed analyses, spectral overlap among fluorophores imposes significant limitations, hindering the realization of high-throughput, parallel real-time monitoring.

2.5. SERS Biosensors

Similar to the principle of surface-enhanced fluorescence, SERS is a detection technique that relies on the localized surface plasmon resonance of metallic nanostructures to markedly amplify Raman signals, offering advantages such as high sensitivity, molecular fingerprinting, and label-free detection [92]. Through its programmable self-assembly capability, DNA origami can precisely organize metallic nanoparticles at the nanoscale to construct highly controllable "hotspot" structures, thereby improving signal uniformity and stability [93–95]. Compared with conventional SERS platforms, this approach not only

enhances detection sensitivity but also opens new avenues for multiplexed analysis and reproducible biosensing.

Some researchers have directed their efforts toward protein detection [96–99]. For example, Heck et al. used DNA origami to self-assemble silver nanoparticles with diameters of 10 nm, 20 nm, and 60 nm into silver nanolenses, selectively integrating streptavidin at the plasmonic hotspots. This approach enabled the detection of the SERS signal from alkyne-labeled streptavidin within a single silver nanolens, thereby offering new opportunities for single-molecule SERS studies of complex biomolecules [100]. Recently, Schuknecht et al. employed a DNA origami template to precisely assemble gold nanorods (AuNRs) into tip-to-tip dimers, creating an accessible hotspot of approximately 8 nm. Using this design, single-molecule detection of streptavidin and thrombin was achieved via SERS, with a detection limit of 0.1 pM—approximately 1000-fold lower than that of conventional SERS-based protein assays—highlighting the high sensitivity and specificity of this method for label-free protein recognition (Figure 5A) [101].

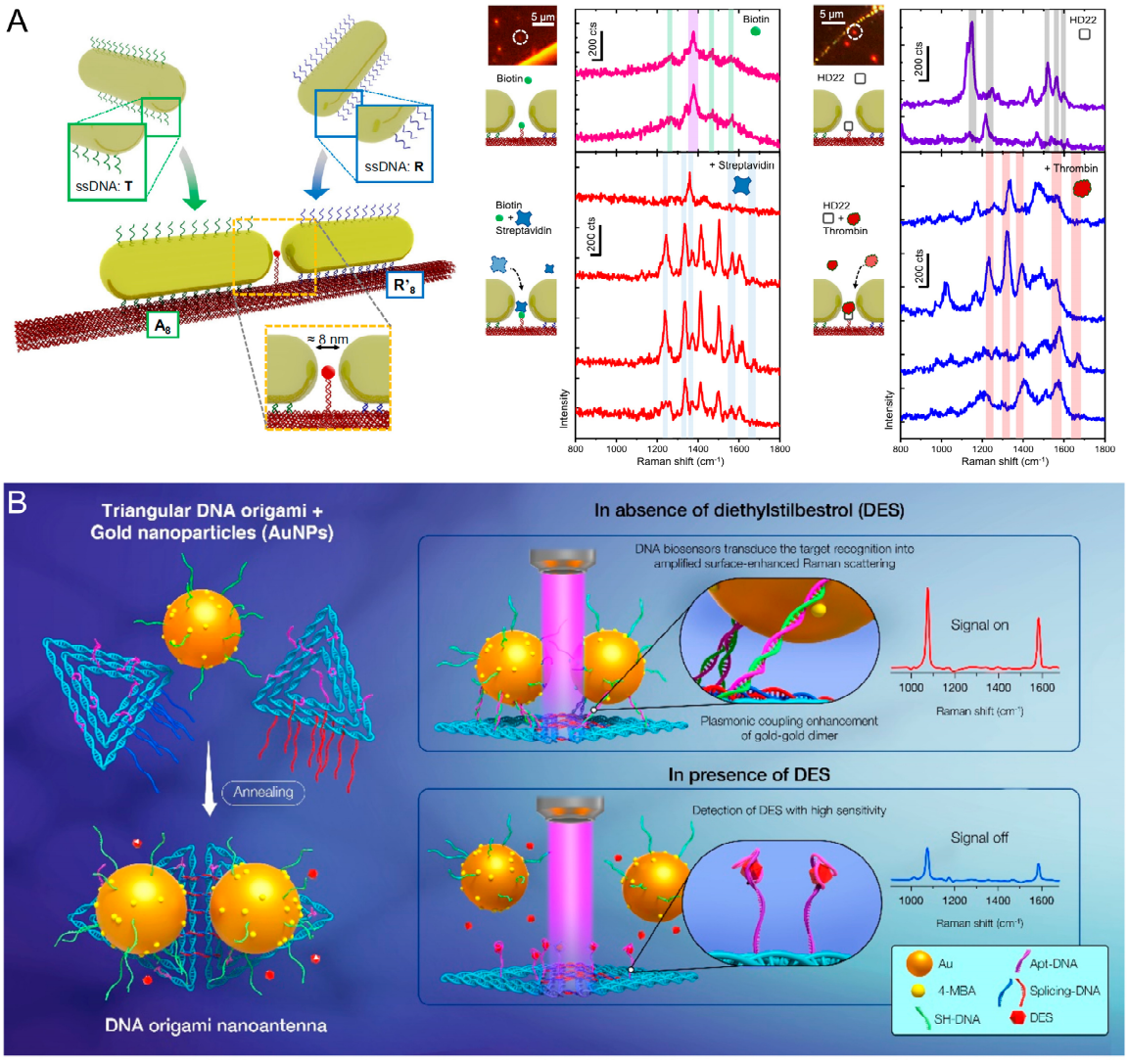


Figure 5. SERS biosensors enabled by DNA origami. (**A**) DNA origami scaffolds were used to assemble plasmonic nanoantennas that generate fluorescence enhancement hotspots for single streptavidin and thrombin detection [101]. Reproduced from Nature Communications, with permission from Nature, 2023. (**B**) DNA origami-based SERS sensor transduces aptamer-binding induced conformational changes into Raman signals for sensitive detection of diethylstilbestrol [103]. Reproduced from Journal of Hazardous Materials, with permission from Elsevier, 2023.

Some studies have also extended beyond protein detection to investigate other substances. For example, Heck et al. examined the mechanism of amorphous carbon formation during SERS measurements on DNA origami-assembled gold and silver nanostructures. By constructing gold and silver dimers as well as silver nanolenses with DNA origami, the authors systematically evaluated the influence of excitation wavelength, laser power density, and substrate conditions on amorphous carbon generation. Their results demonstrated that amorphous carbon is more prone to form on silver nanostructures and under high irradiation power, with the process attributed to the synergistic effects of thermal excitation and plasmon-induced hot electrons [102]. Recently, Li et al. reported the detection of the environmental estrogen diethylstilbestrol (DES). By employing DNA origami to precisely arrange gold nanoparticles at the nanoscale, well-defined "hotspot" structures were constructed, which, in combination with specific aptamers, enabled selective recognition of DES. Upon target binding, conformational changes in the nanoantenna induced a significant alteration in the Raman signal, thereby allowing sensitive detection. The biosensor exhibited a broad linear response over the range of 100 pM–10 μM with a detection limit of 0.217 nM, and demonstrated high selectivity and satisfactory recovery (96.8–110%) in real samples such as milk (Figure 5B) [103].

DNA origami-based SERS biosensors enable ultrasensitive detection with improved reproducibility by precisely engineering plasmonic hotspots, yet challenges remain in stability, fabrication complexity, and signal uniformity. Advancing structural robustness and scalability will be critical for their translation into practical biomedical applications.

2.6. Other Optical Biosensors

Among optical biosensors, fluorescent biosensors and SERS biosensors have been discussed above; in the following section, we introduce several other types of optical biosensors.

Chirality refers to a geometric property of molecules in which their spatial configurations are non-superimposable on their mirror images, and sensors based on chiral signals typically rely on circular dichroism (CD) as the signal transduction mechanism. Chirality-based biosensors can be employed for the detection of a wide range of analytes [104,105]. In 2018, Funck et al. employed a DNA origami template to construct reconfigurable plasmonic chiral nanostructures, where the chiral arrangement of AuNRs generated pronounced CD signals. Binding of the target RNA triggered conformational changes in the structure, leading to detectable variations in the CD spectrum. Targeting a specific RNA sequence from the hepatitis C virus (HCV) genome, this sensor achieves a detection limit as low as 100 pM—approximately 10-fold lower than that of conventional chiroptical CD biosensors (typical detection limit ~1 nM)—and remains stable in serum environments [106]. In 2017, Kuzyk et al. employed DNA origami-assembled reconfigurable chiral plasmonic metamolecules to achieve pH-dependent detection and regulation. By designing pH-responsive triplex DNA "locks," the authors controlled the chiral configurations of AuNRs on the DNA origami scaffold, thereby generating tunable CD signals under different pH conditions (Figure 6A) [107]. In 2018, Zhou et al. developed a dynamic chiral plasmonic nanosystem based on DNA origami. In this work, split aptamers (ATP and cocaine aptamers) were combined with DNA origami-assembled AuNRs, enabling the system to simultaneously respond to temperature variations and target molecule binding. By monitoring CD signal changes, sensitive detection of ATP and cocaine was achieved, with detection limits of 1 μM and 5 μM, respectively—approximately 10–20 times lower than those of conventional chiral plasmonic sensors for these analytes—demonstrating dual responsiveness through the integration of thermal regulation and molecular recognition (Figure 6B) [108].

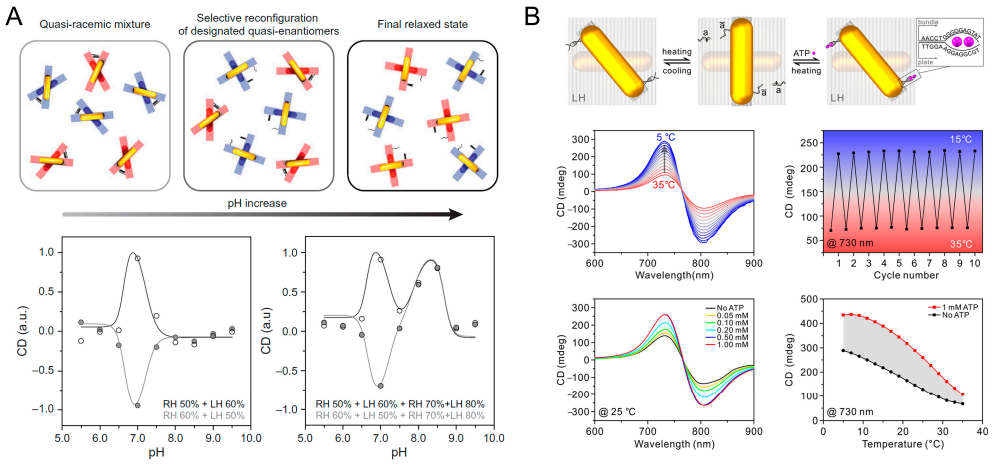


Figure 6. Other optical biosensors enabled by DNA origami. (**A**) DNA origami-assembled AuNR chiral metamolecules detect pH via pH-responsive conformational switching [107]. Reproduced from Science Advances, with permission from The American Association for the Advancement of Science, 2017. (**B**) DNA origami templates arranged crossed AuNRs with split aptamers, where structural switching is regulated by temperature or aptamer-target binding, and read out by CD spectra [108]. Reproduced from Nano Letters, with permission from American Chemical Society, 2018.

DNA origami-based optical biosensors offer high programmability and spatial precision, enabling the ordered arrangement of metallic nanoparticles to enhance detection sensitivity and specificity. However, their stability remains limited in complex biological environments, and the signals are susceptible to environmental noise and structural heterogeneity. In addition, their construction is complex and reliant on advanced instrumentation, making large-scale production and clinical translation challenging.

Surface plasmon resonance (SPR) can also serve as the output signal for biosensors. Daems et al. employed three-dimensional DNA origami structures to precisely arrange bioreceptors at the nanoscale, thereby functionalizing a fiber optic SPR (FO-SPR) sensor. The research team designed DNA origami with different configurations to anchor thrombin-specific aptamers on the sensing surface and systematically investigated their stability, orientation, density, and correlation with sensing performance. The results demonstrated that this strategy not only enables label-free detection of thrombin but also provides improved signal accessibility and a broader linear detection range without the need for the conventional backfilling step, highlighting the unique advantages of DNA origami in constructing high-performance SPR biosensors [109].

As discussed above, various types of DNA origami-based biosensors have been reviewed in detail. To facilitate comprehension, the key quantitative performance indicators of these biosensors are summarized in a comparative format, as presented in Table 1.

Table 1. Comparative summary of key quantitative performance indicators of DNA origami-based biosensors.

Types	Target	Limit of Detection	Linear Range	Sample Matrix	Ref.
Microscopy-Based Biosensors	RNA	200 pM	/	RNA extract (mouse pro-B cells); buffer	[31]
	miRNA-133	/	miRNA/Origami (0–16,000)	synthetic miRNA samples in buffer	[33]
	pH	/	pH 5.0–8.0	buffer; CNT microenvironment	[43]

Table 1. *Cont.*

Types	Target	Limit of Detection	Linear Range	Sample Matrix	Ref.
Nanopore Biosensors	dsDNA, ssDNA	/	ssDNA; 500 nM; λ-DNA: 1 nM	$KCl/MgCl_2$; TBE	[54]
	CRP	3 nM in buffer; 9 nM in 5% human plasma	3 nM–90 nM	KCl; 5% human plasma	[55]
	miRNA-141-3p	nanomolar range	0–200 nM	$KCl/MgCl_2$ buffer; 2% human serum	[56]
Electrochemical Biosensors	miRNA-21	79.8 fM	0.1 pM–10.0 nM	1% human serum	[59]
	blaOXA-1 β-lactamase gene	8.86 pM	10 pM–1 nM	buffer; origami folding mix	[60]
	ctDNA	0.26 fM	1 fM–10 pM	10% human serum	[61]
	streptavidin	<1 pM	5 pM–1 nM	TAE/Mg^{2+} buffer	[62]
Fluorescent Biosensors	ATP	0.10 mM	0.10 mM–1.00 mM ATP	experimental buffer	[76]
	Compressive depletion forces	~40 fN	0–0.61 pN	0.5 × TBE; $MgCl_2$	[82]
	voltage	/	100–600 mV	electrolyte solution	[84]
	pH	0.5 pH unit difference	pH 6.0–8.0	buffer; 1–10% plasma	[83]
	Membrane charges	/	0–80% DOPG	large unilamellar vesicles; 50% plasma	[85]
	miRNA-21, let-7a	1–10 pM	10 pM–1 μM	buffer; miRNA (MCF–7 cells)	[70]
	nanoparticle and vesicle size	36 nm–300 nm	50–300 nm (silica particles); 50–200 nm (lipid vesicles)	buffer; lipid vesicle suspension	[86]
	151-nucleotide sequence	5 aM (buffer); 10 aM (human plasma)	1 aM–5 nM	buffer; untreated human plasma	[91]
SERS Biosensors	diethylstilbestrol	0.217 nM	100 pM–10 μM	Spiked milk; anhydrous methanol	[103]
Chirality-based biosensors	streptavidin, thrombin	single-molecule level	/	water; TE buffer; PBS buffer	[101]
	pH	/	pH 5.5–9.5	different pH buffer systems	[107]
	ATP	/	0.05–1 mM	buffer	[108]
	RNA	100 pM	0–100 nM	buffer; serum	[106]
SPR biosensors	human α-thrombin	11.2 nM	15.5–248 nM	buffer	[109]
ELISA combined with DNA origami	PSA	50 aM	50 aM–5 pM	serum	[110]

3. Conclusions and Outlook

DNA origami, as a multifunctional and programmable nanoscale platform, has expanded the toolkit for biosensing. By enabling precise spatial control of functional molecules at the nanometer scale, DNA origami-based biosensors have demonstrated remarkable improvements in sensitivity, selectivity, and multiplexing capability across diverse detection modes, including microscopy, nanopores, electrochemistry, fluorescence, SERS, and other optical approaches. Beyond these conventional sensing strategies, several

innovative explorations have further highlighted the potential of DNA origami in emerging detection schemes. For example, Yan et al. combined rolling circle amplification (RCA) with DNA origami to construct DNA "nanobelts," which were integrated into a magnetic bead-based ELISA system, achieving ultrasensitive detection of prostate-specific antigen (PSA) [110]. Daems et al. employed DNA origami to precisely arrange aptamers at the nanoscale, enabling single-molecule counting of the peanut allergen Ara h1 in digital microwell arrays, with a limit of detection improved by four orders of magnitude compared to traditional ELISA [111]. Rutten et al. further introduced a three-dimensional DNA origami-tailored bioreceptor immobilization strategy on a microfluidic platform, which significantly enhanced the binding efficiency and signal response of aptamer–thrombin interactions [112]. Meanwhile, Ijäs et al. applied DNA origami to lateral flow immunoassays (LFIA), where molecularly precise control of antibody–label stoichiometry resulted in a 55- to 125-fold increase in the sensitivity for detecting cardiac troponin I [113]. Collectively, these advances underscore the unique advantages of DNA origami in addressing long-standing challenges in biosensing, such as limited spatial resolution, poor reproducibility, and the difficulty of dynamic single-molecule analysis.

Despite these achievements, significant challenges remain before DNA origami-based biosensors can be applied in practical diagnostics. Current limitations include the high cost and complexity of DNA origami fabrication, structural instability under physiological conditions, and difficulties in integrating these nanosystems with portable and user-friendly devices. Moreover, the reproducibility of large-scale manufacturing and the robustness of biosensors in real-world complex environments still need substantial improvement. Furthermore, the validation of DNA origami-based biosensors in real and diverse clinical samples remains limited. To achieve clinical translation, systematic studies using complex biological matrices such as whole blood, urine, and saliva are required. In addition, compliance with international standards for in vitro diagnostics—including reproducibility, stability, sensitivity, and regulatory approval processes—will be indispensable. Addressing these challenges will determine whether DNA origami biosensors can evolve from proof-of-concept devices into clinically reliable diagnostic tools.

To address the high cost of DNA raw materials, several groups have developed large-scale production methods for recombinant phage DNA. By optimizing fermentation conditions, the yield of scaffold DNA has been increased by more than tenfold. In parallel, a combined strategy of solid-phase and enzymatic synthesis has been employed to reduce the cost of staple strands, ultimately lowering the preparation cost of DNA origami from approximately USD 100 to less than USD 30 per milligram [114]. In terms of assembly processes, microfluidic continuous-flow systems have enabled the continuous synthesis of DNA origami. Compared with conventional batch reactions, this approach improves production efficiency by 5–8 times and achieves markedly enhanced structural uniformity (structural deviation < 5%) through precise control of temperature gradients and ionic concentrations [115]. In addition, advances in lyophilization technology have extended the shelf life of DNA origami to over six months at room temperature, effectively addressing challenges in storage and transportation following large-scale production [116]. Nevertheless, the large-scale manufacture of DNA origami structures still faces significant obstacles, including the difficulty of quality control for scaffold DNA and the challenges of implementing functional modifications at scale. These issues directly affect assembly efficiency and the consistency of sensor performance, thereby constraining the commercialization of DNA origami-based biosensors. Despite their many advantages, DNA origami sensors remain 3–5 times more expensive than traditional methods and require sophisticated instrumentation. Furthermore, the lack of sufficient clinical validation data continues to limit their acceptance in the marketplace.

Looking ahead, future efforts should focus on enhancing structural stability through chemical modifications, hybrid nanomaterial integration, and protective coatings, thereby improving biocompatibility and performance in complex media. The development of scalable and cost-effective assembly strategies will be crucial for facilitating clinical and commercial applications. Furthermore, combining DNA origami with emerging technologies—such as machine learning [117]-assisted design, microfluidics [118] for automation, and advanced photonic/electronic readout systems—holds great promise to elevate biosensing toward real-time, multiplexed, and point-of-care diagnostics.

Author Contributions: Writing—original draft preparation, R.N. and M.T.; writing—review and editing, R.N. and J.C.; funding acquisition, R.N. All authors have read and agreed to the published version of the manuscript.

Funding: This work was supported by the National Natural Science Foundation of China (Nos. 62401494).

Conflicts of Interest: The authors declare no conflicts of interest.

Abbreviations

4-MBA	4-Mercaptobenzoic Acid
AFM	Atomic Force Microscopy
ATP	Adenosine Triphosphate
AuNP	Gold Nanoparticle
AuNR	Gold Nanorod
CD	Circular Dichroism
ctDNA	Circulating Tumor DNA
CV	Coefficient of Variation
DES	Diethylstilbestrol
DHP	Dihydropyridine
EIS	Electrochemical Impedance Spectroscopy
FO-SPR	Fiber Optic Surface Plasmon Resonance
FRET	Fluorescence Resonance Energy Transfer
GOx	Glucose Oxidase
HCV	Hepatitis C Virus
HRP	Horseradish Peroxidase
LFIA	Lateral Flow Immunoassay
MB	Methylene Blue
PDGF-BB	Platelet-Derived Growth Factor BB
PEG	Polyethylene Glycol
PNA	Peptide Nucleic Acid
PSA	Prostate-Specific Antigen
RCA	Rolling Circle Amplification
RCT	Charge Transfer Resistance
SEM	Scanning Electron Microscopy
SERS	Surface-Enhanced Raman Spectroscopy
SLE	Systemic Lupus Erythematosus
SNP	Single-Nucleotide Polymorphism
Spd^{3+}	Spermidine
SPR	Surface Plasmon Resonance
SWV	Square Wave Voltammetry
TEM	Transmission Electron Microscopy

References

1. Yang, Z.; Mao, S.; Wang, L.; Fu, S.; Dong, Y.; Jaffrezic-Renault, N.; Guo, Z. CRISPR/Cas and Argonaute-Based Biosensors for Pathogen Detection. *ACS Sens.* **2023**, *8*, 3623–3642. [CrossRef] [PubMed]
2. Liu, R.; Li, J.; Salena, B.J.; Li, Y. Aptamer and Dnazyme Based Colorimetric Biosensors for Pathogen Detection. *Angew. Chem. Int. Ed.* **2025**, *64*, e202418725. [CrossRef]
3. Hwang, M.T.; Heiranian, M.; Kim, Y.; You, S.; Leem, J.; Taqieddin, A.; Faramarzi, V.; Jing, Y.; Park, I.; van der Zande, A.M.; et al. Ultrasensitive Detection of Nucleic Acids Using Deformed Graphene Channel Field Effect Biosensors. *Nat. Commun.* **2020**, *11*, 1543. [CrossRef]
4. Osman, D.I.; El-Sheikh, S.M.; Sheta, S.M.; Ali, O.I.; Salem, A.M.; Shousha, W.G.; El-Khamisy, S.F.; Shawky, S.M. Nucleic Acids Biosensors Based on Metal-Organic Framework (Mof): Paving the Way to Clinical Laboratory Diagnosis. *Biosens. Bioelectron.* **2019**, *141*, 111451. [CrossRef]
5. Zhao, S.; Qiao, X.; Chen, M.; Li, Y.; Wang, X.; Xu, Z.; Wu, Y.; Luo, X. D-Amino Acid-Based Antifouling Peptides for the Construction of Electrochemical Biosensors Capable of Assaying Proteins in Serum with Enhanced Stability. *ACS Sens.* **2022**, *7*, 1740–1746. [CrossRef]
6. Han, X.; Shen, X.; Zhou, Y.; Wang, L.; Ren, Q.; Cai, Y.; Abdi-Ghaleh, R. Terahertz Vibrational Fingerprints Detection of Molecules with Particularly Designed Graphene Biosensors. *Nanomaterials* **2022**, *12*, 3422. [CrossRef]
7. Lin, A.; Che, C.; Jiang, A.; Qi, C.; Glaviano, A.; Zhao, Z.; Zhang, Z.; Liu, Z.; Zhou, Z.; Cheng, Q.; et al. Protein Spatial Structure Meets Artificial Intelligence: Revolutionizing Drug Synergy-Antagonism in Precision Medicine. *Adv. Sci.* **2025**, *12*, e07764. [CrossRef] [PubMed]
8. Jiang, Y.; Wang, J.; Sun, A.; Zhang, H.; Yu, X.; Qin, W.; Ying, W.; Li, Y.; Chang, C.; Wang, X.; et al. The Coming Era of Proteomics-Driven Precision Medicine. *Natl. Sci. Rev.* **2025**, *12*, nwaf278. [CrossRef] [PubMed]
9. Clark, L.C., Jr.; Lyons, C. Electrode Systems for Continuous Monitoring in Cardiovascular Surgery. *Ann. N. Y. Acad. Sci.* **1962**, *102*, 29–45. [CrossRef]
10. Updike, S.J.; Hicks, G.P. The Enzyme Electrode. *Nature* **1967**, *214*, 986–988. [CrossRef]
11. Rocchitta, G.; Spanu, A.; Babudieri, S.; Latte, G.; Madeddu, G.; Galleri, G.; Nuvoli, S.; Bagella, P.; Demartis, M.I.; Fiore, V.; et al. Enzyme Biosensors for Biomedical Applications: Strategies for Safeguarding Analytical Performances in Biological Fluids. *Sensors* **2016**, *16*, 780. [CrossRef] [PubMed]
12. Pullano, S.A.; Greco, M.; Bianco, M.G.; Foti, D.; Brunetti, A.; Fiorillo, A.S. Glucose Biosensors in Clinical Practice: Principles, Limits and Perspectives of Currently Used Devices. *Theranostics* **2022**, *12*, 493–511. [CrossRef] [PubMed]
13. Shi, W.; Friedman, A.K.; Baker, L.A. Nanopore Sensing. *Anal. Chem.* **2017**, *89*, 157–188. [CrossRef]
14. Singh, S.L.; Chauhan, K.; Bharadwaj, A.S.; Kishore, V.; Laux, P.; Luch, A.; Singh, A.V. Polymer Translocation and Nanopore Sequencing: A Review of Advances and Challenges. *Int. J. Mol. Sci.* **2023**, *24*, 6153. [CrossRef] [PubMed]
15. Rothemund, P.W. Folding DNA to Create Nanoscale Shapes and Patterns. *Nature* **2006**, *440*, 297–302. [CrossRef]
16. Zhan, P.; Peil, A.; Jiang, Q.; Wang, D.; Mousavi, S.; Xiong, Q.; Shen, Q.; Shang, Y.; Ding, B.; Lin, C.; et al. Recent Advances in DNA Origami-Engineered Nanomaterials and Applications. *Chem. Rev.* **2023**, *123*, 3976–4050. [CrossRef]
17. He, Z.; Shi, K.; Li, J.; Chao, J. Self-Assembly of DNA Origami for Nanofabrication, Biosensing, Drug Delivery, and Computational Storage. *iScience* **2023**, *26*, 106638. [CrossRef]
18. Marras, A.E.; Zhou, L.; Su, H.J.; Castro, C.E. Programmable Motion of DNA Origami Mechanisms. *Proc. Natl. Acad. Sci. USA* **2015**, *112*, 713–718. [CrossRef]
19. Mourdikoudis, S.; Pallares, R.M.; Thanh, N.T.K. Characterization Techniques for Nanoparticles: Comparison and Complementarity Upon Studying Nanoparticle Properties. *Nanoscale* **2018**, *10*, 12871–12934. [CrossRef]
20. Heath, G.R.; Kots, E.; Robertson, J.L.; Lansky, S.; Khelashvili, G.; Weinstein, H.; Scheuring, S. Localization Atomic Force Microscopy. *Nature* **2021**, *594*, 385–390. [CrossRef]
21. Collins, L.; Liu, Y.; Ovchinnikova, O.S.; Proksch, R. Quantitative Electromechanical Atomic Force Microscopy. *ACS Nano* **2019**, *13*, 8055–8066. [CrossRef] [PubMed]
22. Fan, Z.; Zhang, L.; Baumann, D.; Mei, L.; Yao, Y.; Duan, X.; Shi, Y.; Huang, J.; Huang, Y.; Duan, X. In Situ Transmission Electron Microscopy for Energy Materials and Devices. *Adv. Mater.* **2019**, *31*, 1900608. [CrossRef]
23. Guo, H.; Yulaev, A.; Strelcov, E.; Tselev, A.; Arble, C.; Vladar, A.E.; Villarrubia, J.S.; Kolmakov, A. Probing Electrified Liquid-Solid Interfaces with Scanning Electron Microscopy. *ACS Appl. Mater. Interfaces* **2020**, *12*, 56650–56657. [CrossRef] [PubMed]
24. Lazic, I.; Sachse, C. Obtaining Cryo-Em Structures by Scanning Transmission Electron Microscopy. *Nat. Methods* **2022**, *19*, 1179–1180. [CrossRef]
25. Kuzuya, A.; Sakai, Y.; Yamazaki, T.; Xu, Y.; Komiyama, M. Nanomechanical DNA Origami 'Single-Molecule Beacons' Directly Imaged by Atomic Force Microscopy. *Nat. Commun.* **2011**, *2*, 449. [CrossRef]
26. Lu, Z.; Wang, Y.; Xu, D.; Pang, L. Aptamer-Tagged DNA Origami for Spatially Addressable Detection of Aflatoxin B1. *Chem. Comm.* **2013**, *53*, 941–944. [CrossRef]

27. Liu, K.; Pan, D.; Wen, Y.; Zhang, H.; Chao, J.; Wang, L.; Song, S.; Fan, C.; Shi, Y. Identifying the Genotypes of Hepatitis B Virus (Hbv) with DNA Origami Label. *Small* **2017**, *14*, 1701718. [CrossRef]
28. Godonoga, M.; Lin, T.Y.; Oshima, A.; Sumitomo, K.; Tang, M.S.L.; Cheung, Y.W.; Kinghorn, A.B.; Dirkzwager, R.M.; Zhou, C.; Kuzuya, A.; et al. A DNA Aptamer Recognising a Malaria Protein Biomarker Can Function as Part of a DNA Origami Assembly. *Sci. Rep.* **2016**, *6*, 21266. [CrossRef]
29. Wang, K.; Huang, Q.; Elshaer, M.R.; Knorr, B.; Chaikin, P.; Zhu, G. Tri-State Logic Computation by Activating DNA Origami Chains. *Nanoscale* **2024**, *16*, 11991–11998. [CrossRef] [PubMed]
30. Huang, Q.; Kim, J.; Wang, K.; Vecchioni, S.; Ohayon, Y.P.; Seeman, N.C.; Jonoska, N.; Sha, R. Environmentally Controlled Oscillator with Triplex Guided Displacement of DNA Duplexes. *Nano Lett.* **2023**, *23*, 7593–7598. [CrossRef]
31. Ke, Y.; Lindsay, S.; Chang, Y.; Liu, Y.; Yan, H. Self-Assembled Water-Soluble Nucleic Acid Probe Tiles for Label-Free RNA Hybridization Assays. *Science* **2008**, *319*, 180–183. [CrossRef] [PubMed]
32. Wang, D.; Fu, Y.; Yan, J.; Zhao, B.; Dai, B.; Chao, J.; Liu, H.; He, D.; Zhang, Y.; Fan, C.; et al. Molecular Logic Gates on DNA Origami Nanostructures for Microrna Diagnostics. *Anal. Chem.* **2014**, *86*, 1932–1936. [CrossRef] [PubMed]
33. Zhu, J.; Feng, X.; Lou, J.; Li, W.; Li, S.; Zhu, H.; Yang, L.; Zhang, A.; He, L.; Li, C. Accurate Quantification of Microrna Via Single Strand Displacement Reaction on DNA Origami Motif. *PLoS ONE* **2013**, *8*, e69856. [CrossRef] [PubMed]
34. Kuzuya, A.; Sakai, Y.; Yamazaki, T.; Xu, Y.; Yamanaka, Y.; Ohya, Y.; Komiyama, M. Allosteric Control of Nanomechanical DNA Origami Pinching Devices for Enhanced Target Binding. *Chem. Comm.* **2017**, *53*, 8276–8279. [CrossRef]
35. Zhang, Z.; Wang, Y.; Fan, C.; Li, C.; Li, Y.; Qian, L.; Fu, Y.; Shi, Y.; Hu, J.; He, L. Asymmetric DNA Origami for Spatially Addressable and Index-Free Solution-Phase DNA Chips. *Adv. Mater.* **2010**, *22*, 2672–2675. [CrossRef]
36. Torelli, E.; Marini, M.; Palmano, S.; Piantanida, L.; Polano, C.; Scarpellini, A.; Lazzarino, M.; Firrao, G. A DNA Origami Nanorobot Controlled by Nucleic Acid Hybridization. *Small* **2014**, *10*, 2918–2926. [CrossRef]
37. Xiong, J.; He, Z.; Wang, L.; Fan, C.; Chao, J. DNA Origami-Enabled Gene Localization of Repetitive Sequences. *J. Am. Chem. Soc.* **2024**, *146*, 6317–6325. [CrossRef]
38. Hosseini Aghouzi, S.M.; Yildiz, E.; Mordogan, F.; Erdem, A. Biosensing of Single-Nucleotide Polymorphism: Technological Advances and Their Transformative Applications on Health. *Biosens. Bioelectron.* **2025**, *279*, 117385. [CrossRef]
39. Zhang, Z.; Zeng, D.; Ma, H.; Feng, G.; Hu, J.; He, L.; Li, C.; Fan, C. A DNA-Origami Chip Platform for Label-Free Snp Genotyping Using Toehold-Mediated Strand Displacement. *Small* **2010**, *6*, 1854–1858. [CrossRef]
40. Subramanian, H.K.; Chakraborty, B.; Sha, R.; Seeman, N.C. The Label-Free Unambiguous Detection and Symbolic Display of Single Nucleotide Polymorphisms on DNA Origami. *Nano Lett.* **2011**, *11*, 910–913. [CrossRef]
41. Zhang, H.; Chao, J.; Pan, D.; Liu, H.; Qiang, Y.; Liu, K.; Cui, C.; Chen, J.; Huang, Q.; Hu, J.; et al. DNA Origami-Based Shape Ids for Single-Molecule Nanomechanical Genotyping. *Nat. Commun.* **2017**, *8*, 14738. [CrossRef]
42. Kuzuya, A.; Watanabe, R.; Yamanaka, Y.; Tamaki, T.; Kaino, M.; Ohya, Y. Nanomechanical DNA Origami Ph Sensors. *Sensors* **2014**, *14*, 19329–19335. [CrossRef]
43. Zhang, X.; Pan, L.; Guo, R.; Zhang, Y.; Li, F.; Li, M.; Li, J.; Shi, J.; Qu, F.; Zuo, X.; et al. DNA Origami Nanocalipers for Ph Sensing at the Nanoscale. *Chem. Comm.* **2022**, *58*, 3673–3676. [CrossRef]
44. Wang, X.; Li, C.; Niu, D.; Sha, R.; Seeman, N.C.; Canary, J.W. Construction of a DNA Origami Based Molecular Electro-Optical Modulator. *Nano Lett.* **2018**, *18*, 2112–2115. [CrossRef] [PubMed]
45. Voigt, N.V.; Torring, T.; Rotaru, A.; Jacobsen, M.F.; Ravnsbaek, J.B.; Subramani, R.; Mamdouh, W.; Kjems, J.; Mokhir, A.; Besenbacher, F.; et al. Single-Molecule Chemical Reactions on DNA Origami. *Nat. Nanotechnol.* **2010**, *5*, 200–203. [CrossRef]
46. Tintore, M.; Gallego, I.; Manning, B.; Eritja, R.; Fabrega, C. DNA Origami as a DNA Repair Nanosensor at the Single-Molecule Level. *Angew. Chem. Int. Ed.* **2013**, *52*, 7747–7750. [CrossRef]
47. Endo, M.; Sugiyama, H. Single-Molecule Imaging of Dynamic Motions of Biomolecules in DNA Origami Nanostructures Using High-Speed Atomic Force Microscopy. *Acc. Chem. Res.* **2014**, *47*, 1645–1653. [CrossRef]
48. Prakash, P.S.; Joshi, F.M.; Vogelsberg, E.; Cremers, G.A.O.; Gur, F.N.; Sato, Y.; de Greef, T.F.A.; Ader, M.; Kurth, T.; Nunes Goncalves, D.P.; et al. DNA Origami Barcodes for Immunostaining. *ACS Appl. Mater. Interfaces* **2025**, *17*, 15813–15823. [CrossRef] [PubMed]
49. Spitzberg, J.D.; Zrehen, A.; van Kooten, X.F.; Meller, A. Plasmonic-Nanopore Biosensors for Superior Single-Molecule Detection. *Adv. Mater.* **2019**, *31*, e1900422. [CrossRef] [PubMed]
50. Zhang, H.; Zhao, T.; Huang, P.; Wang, Q.; Tang, H.; Chu, X.; Jiang, J. Spatiotemporally Resolved Protein Detection in Live Cells Using Nanopore Biosensors. *ACS Nano* **2022**, *16*, 5752–5763. [CrossRef]
51. Bell, N.A.; Engst, C.R.; Ablay, M.; Divitini, G.; Ducati, C.; Liedl, T.; Keyser, U.F. DNA Origami Nanopores. *Nano Lett.* **2012**, *12*, 512–517. [CrossRef]
52. Wei, R.; Martin, T.G.; Rant, U.; Dietz, H. DNA Origami Gatekeepers for Solid-State Nanopores. *Angew. Chem. Int. Ed.* **2012**, *51*, 4864–4867. [CrossRef]

53. Barati Farimani, A.; Dibaeinia, P.; Aluru, N.R. DNA Origami-Graphene Hybrid Nanopore for DNA Detection. *ACS Appl. Mater. Interfaces* **2017**, *9*, 92–100. [CrossRef]
54. Hernandez-Ainsa, S.; Bell, N.A.; Thacker, V.V.; Gopfrich, K.; Misiunas, K.; Fuentes-Perez, M.E.; Moreno-Herrero, F.; Keyser, U.F. DNA Origami Nanopores for Controlling DNA Translocation. *ACS Nano* **2013**, *7*, 6024–6030. [CrossRef]
55. Raveendran, M.; Lee, A.J.; Sharma, R.; Walti, C.; Actis, P. Rational Design of DNA Nanostructures for Single Molecule Biosensing. *Nat. Commun.* **2020**, *11*, 4384. [CrossRef] [PubMed]
56. Long, L.; Johnson, J.A.; Ren, R.; Michele, L.D.; Edel, J.B.; Ivanov, A.P. Reconfigurable DNA Origami Hinges for Nanopore Detection of Microrna. *Nano Res.* **2025**, *18*, 94907604. [CrossRef]
57. Wu, J.; Liu, H.; Chen, W.; Ma, B.; Ju, H. Device Integration of Electrochemical Biosensors. *Nat. Rev. Bioeng.* **2023**, *1*, 346–360. [CrossRef]
58. Du, X.; Zhang, Z.; Zheng, X.; Zhang, H.; Dong, D.; Zhang, Z.; Liu, M.; Zhou, J. An Electrochemical Biosensor for the Detection of Epithelial-Mesenchymal Transition. *Nat. Commun.* **2020**, *11*, 192. [CrossRef]
59. Han, S.; Liu, W.; Yang, S.; Wang, R. Facile and Label-Free Electrochemical Biosensors for Microrna Detection Based on DNA Origami Nanostructures. *ACS Omega* **2019**, *4*, 11025–11031. [CrossRef] [PubMed]
60. Williamson, P.; Piskunen, P.; Ijas, H.; Butterworth, A.; Linko, V.; Corrigan, D.K. Signal Amplification in Electrochemical DNA Biosensors Using Target-Capturing DNA Origami Tiles. *ACS Sens.* **2023**, *8*, 1471–1480. [CrossRef]
61. Qin, W.; Gong, X.; Duan, X.; Hao, J.; Ren, H.; ShenTu, X.; Ye, Z.; Yu, X. Supercharged DNA Origami Enhanced Signal Amplification for Ultrasensitive Detection of Nucleic Acid. *Biosens. Bioelectron.* **2025**, *287*, 117692. [CrossRef]
62. Jeon, B.J.; Guareschi, M.M.; Stewart, J.M.; Wu, E.; Gopinath, A.; Arroyo-Curras, N.; Dauphin-Ducharme, P.; Plaxco, K.W.; Lukeman, P.S.; Rothemund, P.W.K. Modular DNA Origami-Based Electrochemical Detection of DNA and Proteins. *Proc. Natl. Acad. Sci. USA* **2025**, *122*, e2311279121. [CrossRef]
63. Ge, Z.; Fu, J.; Liu, M.; Jiang, S.; Andreoni, A.; Zuo, X.; Liu, Y.; Yan, H.; Fan, C. Constructing Submonolayer DNA Origami Scaffold on Gold Electrode for Wiring of Redox Enzymatic Cascade Pathways. *ACS Appl. Mater. Interfaces* **2019**, *11*, 13881–13887. [CrossRef]
64. Metternich, J.T.; Wartmann, J.A.C.; Sistemich, L.; Nissler, R.; Herbertz, S.; Kruss, S. Near-Infrared Fluorescent Biosensors Based on Covalent DNA Anchors. *J. Am. Chem. Soc.* **2023**, *145*, 14776–14783. [CrossRef]
65. Guisan-Ceinos, S.; Rivero, A.R.; Romeo-Gella, F.; Simon-Fuente, S.; Gomez-Pastor, S.; Calvo, N.; Orrego, A.H.; Guisan, J.M.; Corral, I.; Sanz-Rodriguez, F.; et al. Turn-on Fluorescent Biosensors for Imaging Hypoxia-Like Conditions in Living Cells. *J. Am. Chem. Soc.* **2022**, *144*, 8185–8193. [CrossRef]
66. Krause, S.; Ploetz, E.; Bohlen, J.; Schuler, P.; Yaadav, R.; Selbach, F.; Steiner, F.; Kaminska, I.; Tinnefeld, P. Graphene-on-Glass Preparation and Cleaning Methods Characterized by Single-Molecule DNA Origami Fluorescent Probes and Raman Spectroscopy. *ACS Nano* **2021**, *15*, 6430–6438. [CrossRef]
67. Mathur, D.; Henderson, E.R. Programmable DNA Nanosystem for Molecular Interrogation. *Sci. Rep.* **2016**, *6*, 27413. [CrossRef]
68. Selnihhin, D.; Sparvath, S.M.; Preus, S.; Birkedal, V.; Andersen, E.S. Multifluorophore DNA Origami Beacon as a Biosensing Platform. *ACS Nano* **2018**, *12*, 5699–5708. [CrossRef] [PubMed]
69. Zadegan, R.M.; Jepsen, M.D.; Thomsen, K.E.; Okholm, A.H.; Schaffert, D.H.; Andersen, E.S.; Birkedal, V.; Kjems, J. Construction of a 4 Zeptoliters Switchable 3D DNA Box Origami. *ACS Nano* **2012**, *6*, 10050–10053. [CrossRef] [PubMed]
70. Domljanovic, I.; Loretan, M.; Kempter, S.; Acuna, G.P.; Kocabey, S.; Ruegg, C. DNA Origami Book Biosensor for Multiplex Detection of Cancer-Associated Nucleic Acids. *Nanoscale* **2022**, *14*, 15432–15441. [CrossRef] [PubMed]
71. Domljanovic, I.; Carstens, A.; Okholm, A.; Kjems, J.; Nielsen, C.T.; Heegaard, N.H.H.; Astakhova, K. Complexes of DNA with Fluorescent Dyes Are Effective Reagents for Detection of Autoimmune Antibodies. *Sci. Rep.* **2017**, *7*, 1925. [CrossRef]
72. Tang, M.S.L.; Shiu, S.C.; Godonoga, M.; Cheung, Y.W.; Liang, S.; Dirkzwager, R.M.; Kinghorn, A.B.; Fraser, L.A.; Heddle, J.G.; Tanner, J.A. An Aptamer-Enabled DNA Nanobox for Protein Sensing. *Nanomedicine* **2018**, *14*, 1161–1168. [CrossRef]
73. Ke, Y.; Meyer, T.; Shih, W.M.; Bellot, G. Regulation at a Distance of Biomolecular Interactions Using a DNA Origami Nanoactuator. *Nat. Commun.* **2016**, *7*, 10935. [CrossRef] [PubMed]
74. Domljanovic, I.; Rexen Ulven, E.; Ulven, T.; Thomsen, R.P.; Okholm, A.H.; Kjems, J.; Voss, A.; Taskova, M.; Astakhova, K. Dihydropyridine Fluorophores Allow for Specific Detection of Human Antibodies in Serum. *ACS Omega* **2018**, *3*, 7580–7586. [CrossRef]
75. Wang, X.; Mao, Z.; Chen, R.; Li, S.; Ren, S.; Liang, J.; Gao, Z. Self-Assembled DNA Origami-Based Duplexed Aptasensors Combined with Centrifugal Filters for Efficient and Rechargeable Atp Detection. *Biosens. Bioelectron.* **2022**, *211*, 114336. [CrossRef] [PubMed]
76. Walter, H.K.; Bauer, J.; Steinmeyer, J.; Kuzuya, A.; Niemeyer, C.M.; Wagenknecht, H.A. "DNA Origami Traffic Lights" with a Split Aptamer Sensor for a Bicolor Fluorescence Readout. *Nano Lett.* **2017**, *17*, 2467–2472. [CrossRef]
77. Marras, A.E.; Shi, Z.; Lindell, M.G., 3rd; Patton, R.A.; Huang, C.M.; Zhou, L.; Su, H.J.; Arya, G.; Castro, C.E. Cation-Activated Avidity for Rapid Reconfiguration of DNA Nanodevices. *ACS Nano* **2018**, *12*, 9484–9494. [CrossRef] [PubMed]

78. Grabenhorst, L.; Pfeiffer, M.; Schinkel, T.; Kummerlin, M.; Bruggenthies, G.A.; Maglic, J.B.; Selbach, F.; Murr, A.T.; Tinnefeld, P.; Glembockyte, V. Engineering Modular and Tunable Single-Molecule Sensors by Decoupling Sensing from Signal Output. *Nat. Nanotechnol.* **2025**, *20*, 303–310. [CrossRef]
79. Choi, Y.; Kotthoff, L.; Olejko, L.; Resch-Genger, U.; Bald, I. DNA Origami-Based Forster Resonance Energy-Transfer Nanoarrays and Their Application as Ratiometric Sensors. *ACS Appl. Mater. Interfaces* **2018**, *10*, 23295–23302. [CrossRef]
80. Kaminska, I.; Bohlen, J.; Rocchetti, S.; Selbach, F.; Acuna, G.P.; Tinnefeld, P. Distance Dependence of Single-Molecule Energy Transfer to Graphene Measured with DNA Origami Nanopositioners. *Nano Lett.* **2019**, *19*, 4257–4262. [CrossRef]
81. Vietz, C.; Schütte, M.L.; Wei, Q.; Richter, L.; Lalkens, B.; Ozcan, A.; Tinnefeld, P.; Acuna, G.P. Benchmarking Smartphone Fluorescence-Based Microscopy with DNA Origami Nanobeads: Reducing the Gap toward Single-Molecule Sensitivity. *ACS Omega* **2019**, *4*, 637–642. [CrossRef]
82. Hudoba, M.W.; Luo, Y.; Zacharias, A.; Poirier, M.G.; Castro, C.E. Dynamic DNA Origami Device for Measuring Compressive Depletion Forces. *ACS Nano* **2017**, *11*, 6566–6573. [CrossRef]
83. Ijas, H.; Hakaste, I.; Shen, B.; Kostiainen, M.A.; Linko, V. Reconfigurable DNA Origami Nanocapsule for Ph-Controlled Encapsulation and Display of Cargo. *ACS Nano* **2019**, *13*, 5959–5967. [CrossRef]
84. Hemmig, E.A.; Fitzgerald, C.; Maffeo, C.; Hecker, L.; Ochmann, S.E.; Aksimentiev, A.; Tinnefeld, P.; Keyser, U.F. Optical Voltage Sensing Using DNA Origami. *Nano Lett.* **2018**, *18*, 1962–1971. [CrossRef]
85. Ochmann, S.E.; Schroder, T.; Schulz, C.M.; Tinnefeld, P. Quantitative Single-Molecule Measurements of Membrane Charges with DNA Origami Sensors. *Anal. Chem.* **2022**, *94*, 2633–2640. [CrossRef]
86. Buber, E.; Schroder, T.; Scheckenbach, M.; Dass, M.; Franquelim, H.G.; Tinnefeld, P. DNA Origami Curvature Sensors for Nanoparticle and Vesicle Size Determination with Single-Molecule Fret Readout. *ACS Nano* **2023**, *17*, 3088–3097. [CrossRef]
87. Vietz, C.; Lalkens, B.; Acuna, G.P.; Tinnefeld, P. Synergistic Combination of Unquenching and Plasmonic Fluorescence Enhancement in Fluorogenic Nucleic Acid Hybridization Probes. *Nano Lett.* **2017**, *17*, 6496–6500. [CrossRef]
88. Ochmann, S.E.; Vietz, C.; Trofymchuk, K.; Acuna, G.P.; Lalkens, B.; Tinnefeld, P. Optical Nanoantenna for Single Molecule-Based Detection of Zika Virus Nucleic Acids without Molecular Multiplication. *Anal. Chem.* **2017**, *89*, 13000–13007. [CrossRef] [PubMed]
89. Trofymchuk, K.; Glembockyte, V.; Grabenhorst, L.; Steiner, F.; Vietz, C.; Close, C.; Pfeiffer, M.; Richter, L.; Schutte, M.L.; Selbach, F.; et al. Addressable Nanoantennas with Cleared Hotspots for Single-Molecule Detection on a Portable Smartphone Microscope. *Nat. Commun.* **2021**, *12*, 950. [CrossRef] [PubMed]
90. Ghamari, S.; Chiarelli, G.; Kolataj, K.; Subramanian, S.; Acuna, G.P.; Vollmer, F. Label-Free (Fluorescence-Free) Sensing of a Single DNA Molecule on DNA Origami Using a Plasmon-Enhanced Wgm Sensor. *Nanophotonics* **2025**, *14*, 253–262. [CrossRef] [PubMed]
91. Yaadav, R.; Trofymchuk, K.; Dass, M.; Behrendt, V.; Hauer, B.; Schutz, J.; Close, C.; Scheckenbach, M.; Ferrari, G.; Maurer, L.; et al. Bringing Attomolar Detection to the Point-of-Care with Nanopatterned DNA Origami Nanoantennas. *Adv. Mater.* **2025**, e07407. [CrossRef]
92. Langer, J.; Jimenez de Aberasturi, D.; Aizpurua, J.; Alvarez-Puebla, R.A.; Auguie, B.; Baumberg, J.J.; Bazan, G.C.; Bell, S.E.J.; Boisen, A.; Brolo, A.G.; et al. Present and Future of Surface-Enhanced Raman Scattering. *ACS Nano* **2020**, *14*, 28–117. [CrossRef]
93. Sharma, M.; Kaur, C.; Singhmar, P.; Rai, S.; Sen, T. DNA Origami-Templated Gold Nanorod Dimer Nanoantennas: Enabling Addressable Optical Hotspots for Single Cancer Biomarker Sers Detection. *Nanoscale* **2024**, *16*, 15128–15140. [CrossRef] [PubMed]
94. Kanehira, Y.; Kogikoski, S., Jr.; Titov, E.; Tapio, K.; Mostafa, A.; Bald, I. Watching a Single Enzyme at Work Using Single-Molecule Surface-Enhanced Raman Scattering and DNA Origami-Based Plasmonic Antennas. *ACS Nano* **2024**, *18*, 20191–20200. [CrossRef]
95. Mostafa, A.; Kanehira, Y.; Tapio, K.; Bald, I. From Bulk to Single Molecules: Surface-Enhanced Raman Scattering of Cytochrome C Using Plasmonic DNA Origami Nanoantennas. *Nano Lett.* **2024**, *24*, 6916–6923. [CrossRef] [PubMed]
96. Tapio, K.; Mostafa, A.; Kanehira, Y.; Suma, A.; Dutta, A.; Bald, I. A Versatile DNA Origami-Based Plasmonic Nanoantenna for Label-Free Single-Molecule Surface-Enhanced Raman Spectroscopy. *ACS Nano* **2021**, *15*, 7065–7077. [CrossRef]
97. Tanwar, S.; Kaur, V.; Kaur, G.; Sen, T. Broadband Sers Enhancement by DNA Origami Assembled Bimetallic Nanoantennas with Label-Free Single Protein Sensing. *J. Phys. Chem. Lett.* **2021**, *12*, 8141–8150. [CrossRef]
98. Dutta, A.; Tapio, K.; Suma, A.; Mostafa, A.; Kanehira, Y.; Carnevale, V.; Bussi, G.; Bald, I. Molecular States and Spin Crossover of Hemin Studied by DNA Origami Enabled Single-Molecule Surface-Enhanced Raman Scattering. *Nanoscale* **2022**, *14*, 16467–16478. [CrossRef]
99. Kaur, C.; Kaur, V.; Rai, S.; Sharma, M.; Sen, T. Selective Recognition of the Amyloid Marker Single Thioflavin T Using DNA Origami-Based Gold Nanobipyramid Nanoantennas. *Nanoscale* **2023**, *15*, 6170–6178. [CrossRef] [PubMed]
100. Heck, C.; Kanehira, Y.; Kneipp, J.; Bald, I. Placement of Single Proteins within the Sers Hot Spots of Self-Assembled Silver Nanolenses. *Angew. Chem. Int. Ed.* **2018**, *57*, 7444–7447. [CrossRef] [PubMed]
101. Schuknecht, F.; Kolataj, K.; Steinberger, M.; Liedl, T.; Lohmueller, T. Accessible Hotspots for Single-Protein Sers in DNA-Origami Assembled Gold Nanorod Dimers with Tip-to-Tip Alignment. *Nat. Commun.* **2023**, *14*, 7192. [CrossRef]
102. Heck, C.; Kanehira, Y.; Kneipp, J.; Bald, I. Amorphous Carbon Generation as a Photocatalytic Reaction on DNA-Assembled Gold and Silver Nanostructures. *Molecules* **2019**, *24*, 2324. [CrossRef]

103. Li, S.; Shi, B.; He, D.; Zhou, H.; Gao, Z. DNA Origami-Mediated Plasmonic Dimer Nanoantenna-Based Sers Biosensor for Ultrasensitive Determination of Trace Diethylstilbestrol. *J. Hazard. Mater.* **2023**, *458*, 131874. [CrossRef] [PubMed]
104. Huang, Y.; Nguyen, M.K.; Natarajan, A.K.; Nguyen, V.H.; Kuzyk, A. A DNA Origami-Based Chiral Plasmonic Sensing Device. *ACS Appl. Mater. Interfaces* **2018**, *10*, 44221–44225. [CrossRef]
105. Funck, T.; Liedl, T.; Bae, W. Dual Aptamer-Functionalized 3D Plasmonic Metamolecule for Thrombin Sensing. *Appl. Sci.* **2019**, *9*, 3006. [CrossRef]
106. Funck, T.; Nicoli, F.; Kuzyk, A.; Liedl, T. Sensing Picomolar Concentrations of RNA Using Switchable Plasmonic Chirality. *Angew. Chem. Int. Ed.* **2018**, *57*, 13495–13498. [CrossRef]
107. Kuzyk, A.; Urban, M.J.; Idili, A.; Ricci, F.; Liu, N. Selective Control of Reconfigurable Chiral Plasmonic Metamolecules. *Sci. Adv.* **2017**, *3*, e1602803. [CrossRef] [PubMed]
108. Zhou, C.; Xin, L.; Duan, X.; Urban, M.J.; Liu, N. Dynamic Plasmonic System That Responds to Thermal and Aptamer-Target Regulations. *Nano Lett.* **2018**, *18*, 7395–7399. [CrossRef] [PubMed]
109. Daems, D.; Pfeifer, W.; Rutten, I.; Sacca, B.; Spasic, D.; Lammertyn, J. Three-Dimensional DNA Origami as Programmable Anchoring Points for Bioreceptors in Fiber Optic Surface Plasmon Resonance Biosensing. *ACS Appl. Mater. Interfaces* **2018**, *10*, 23539–23547. [CrossRef]
110. Yan, J.; Hu, C.; Wang, P.; Liu, R.; Zuo, X.; Liu, X.; Song, S.; Fan, C.; He, D.; Sun, G. Novel Rolling Circle Amplification and DNA Origami-Based DNA Belt-Involved Signal Amplification Assay for Highly Sensitive Detection of Prostate-Specific Antigen (Psa). *ACS Appl. Mater. Interfaces* **2014**, *6*, 20372–20377. [CrossRef]
111. Daems, D.; Rutten, I.; Bath, J.; Decrop, D.; Van Gorp, H.; Ruiz, E.P.; De Feyter, S.; Turberfield, A.J.; Lammertyn, J. Controlling the Bioreceptor Spatial Distribution at the Nanoscale for Single Molecule Counting in Microwell Arrays. *ACS Sens.* **2019**, *4*, 2327–2335. [CrossRef] [PubMed]
112. Rutten, I.; Daems, D.; Lammertyn, J. Boosting Biomolecular Interactions through DNA Origami Nano-Tailored Biosensing Interfaces. *J. Mater. Chem. B* **2020**, *8*, 3606–3615. [CrossRef]
113. Ijas, H.; Trommler, J.; Nguyen, L.; van Rest, S.; Nickels, P.C.; Liedl, T.; Urban, M.J. DNA Origami Signal Amplification in Lateral Flow Immunoassays. *Nat. Commun.* **2025**, *16*, 3216. [CrossRef]
114. Jia, Y.L.; Chen, L.M.; Liu, J.; Li, W.; Gu, H.Z. DNA-Catalyzed Efficient Production of Single-Stranded DNA Nanostructures. *Chem* **2021**, *7*, 959–981. [CrossRef]
115. Ling, Y.F.; Qin, X.; Sun, W.J.; Yue, F.; Wang, Y.W.; Fan, D.; Xu, H.Y.; Xie, R.O.; Zhang, J.W.; Li, J.W.; et al. Precision-Arranged DNA Origami Plasmonic Nanoantennas for Multidimensional Smart-Warning of Weightlessness Induced Bone Loss. *Adv. Sci.* **2025**, e07189. [CrossRef] [PubMed]
116. Xin, Y.; Kielar, C.; Zhu, S.Q.; Sikeler, C.; Xu, X.D.; Moser, C.; Grundmeier, G.; Liedl, T.; Heuer-Jungemann, A.; Smith, D.M.; et al. Cryopreservation of DNA Origami Nanostructures. *Small* **2020**, *16*, 1905959. [CrossRef] [PubMed]
117. Schon, J.C. Enhancing Synthesis Prediction Via Machine Learning. *Nat. Comput. Sci.* **2025**, *5*, 95–96. [CrossRef]
118. Hur, J.; Chung, A.J. Microfluidic and Nanofluidic Intracellular Delivery. *Adv. Sci.* **2021**, *8*, e2004595. [CrossRef]

Disclaimer/Publisher's Note: The statements, opinions and data contained in all publications are solely those of the individual author(s) and contributor(s) and not of MDPI and/or the editor(s). MDPI and/or the editor(s) disclaim responsibility for any injury to people or property resulting from any ideas, methods, instructions or products referred to in the content.